



CHALMERS
UNIVERSITY OF TECHNOLOGY

Food contact of paper and plastic products containing SiO₂, Cu-Phthalocyanine, Fe₂O₃, CaCO₃: Ranking factors that control the

Downloaded from: <https://research.chalmers.se>, 2022-07-02 09:25 UTC

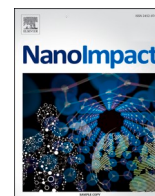
Citation for the original published paper (version of record):

Ruggiero, E., Santizo, K., Persson, M. et al (2022). Food contact of paper and plastic products containing SiO₂, Cu-Phthalocyanine, Fe₂O₃, CaCO₃:

Ranking factors that control the similarity of form and rate of release. NanoImpact, 25.

<http://dx.doi.org/10.1016/j.impact.2021.100372>

N.B. When citing this work, cite the original published paper.



VSI: Similarity of Nanoforms



Food contact of paper and plastic products containing SiO₂, Cu-Phthalocyanine, Fe₂O₃, CaCO₃: Ranking factors that control the similarity of form and rate of release

Emmanuel Ruggiero^{a,d,1}, Katherine Y. Santizo^{a,e,1}, Michael Persson^{b,f}, Camilla Delpivo^c, Wendel Wohlleben^{a,g,*}

^a BASF SE, Dept. Material Physics, 67056 Ludwigshafen, Germany

^b Nouryon Pulp and Performance Chemicals AB, S-445 80 Bohus, Sweden

^c LEITAT Technological Center, C/Pallars 179-185, 08005 Barcelona, Spain

^d Avient, Milano, Italy

^e Virginia Tech, Blacksburg, VA USA

^f Chalmers Industriteknik Sven Hultins Plats 1, S-412 58 Gothenburg, Sweden

^g BASF SE, Dept. Experimental Toxicology and Ecology, 67056 Ludwigshafen, Germany

ARTICLE INFO

Editor: Bernd Nowack

Keywords:

Release
Food contact
Similarity
Cardboard
Plastics
Pigments

ABSTRACT

The paper industry is an important sector annually consuming kilotons of nanoforms and non-nanoforms of fillers and pigments. Fillers accelerate the rate of drying (less energy needed) and product cost (increasing the load of low-cost fillers). The plastic industry is another use sector, where coloristic pigments can be in nanoform, and many food containers are made of plastic. Use of paper to wrap both wet and dry food is consumer practice, but not always intended by producers. Here we compare the release behavior of different nano-enabled products (NEPs) by changing a) nanoform (NF) characteristics, b) NF load, c) the nano-enabled product (NEP) matrix, and d) food simulants. The ranking of these factors enables an assessment of food contact by concepts of analogy, specifically via the similarities of the rate and form of release in food during contact. Three types of matrices were used: Paper, plastic ((Polylactic Acid (PLA), Polyamide (PA6), and Polyurethane (PU)), and a paint formulation. Two nanoforms each of SiO₂, Fe₂O₃, Cu-Phthalocyanine were incorporated, additionally to the conventional form of CaCO₃ that is always contained in paper to reduce cellulose consumption. Tests were guided by the European Regulation EC 1935/2004 and EU 10/2011. No evidence of *particle* release was observed: the *qualitative* similarity (the form of release) was high regarding the food contact of all NEPs with embedded NFs. *Quantitative* similarity of releases depended primarily on the NEP matrix, as this controls the penetration of the simulant fluid into the NEP. The solubility of the NF and impurities in the simulant fluid was the second decisive factor, as dissolution of the NF inside the NEP is the main mechanism of release. This led to complete removal of CaCO₃ in acidic medium, whereas Fe and Si signals remained in the paper, consistent with the low release rates in an ionic form. In our set of 16 NEPs, only one NEP showed a dependence on the REACH NF descriptors (substance, size, shape, surface treatment, crystallinity, impurities), specifically attributed to differences in soluble impurities, whereas for all others the *substance* of the nanoform was sufficient to predict a similarity of food contact release, without influences of size, shape, surface treatment and crystallinity.

1. Introduction

Nanomaterials that are used as fillers and pigments dominate the inventory of nanomaterial production volumes in Europe. (Ministère de

l'Environnement, D. L. É. E. D. L. M, 2015) Nano-enabled products (NEPs) can be created by adding NFs to product matrices to achieve superior performance characteristics such as: durability, coloristic appearance, electrical conductivity, flame resistance, barrier

* Corresponding author.

E-mail address: wendel.wohlleben@basf.com (W. Wohlleben).

¹ Contributed equally.

<https://doi.org/10.1016/j.impact.2021.100372>

Received 29 September 2021; Received in revised form 24 November 2021; Accepted 30 November 2021

Available online 9 December 2021

2452-0748/© 2021 The Author(s).

Published by Elsevier B.V. This is an open access article under the CC BY-NC-ND license

(<http://creativecommons.org/licenses/by-nc-nd/4.0/>).

properties, flexibility, or recycling properties. These are established in many industry segments, including but not limited to: electronics, automotive parts, packaging, paints, coatings, paper, construction, cosmetics, and food.(Stark et al., 2015; Wohlleben et al., 2017) The demonstration of safe use of NEPs as food contact materials (FCM) is challenged by 1) literature of release testing having a narrow focus on polymer-based-NEPs, 2) the regulatory concept of “nanofoms”, raising the question if different grades of the same substance may also differ in the quality or quantity of releases, and 3) the lack of comparative studies that systematically compare releases of the same nanomaterial from different NEP matrices, or that compare releases of different nanomaterial from the same NEP matrix. Our present study aims to fill these gaps.

The general concerns about the release of nanomaterials from NEPs throughout their entire life cycle have been addressed quite substantially on NEPs based on a polymer matrix,(Duncan, 2014; Harper et al., 2015; Froggett et al., 2014) and occasionally matrices other than polymer, such as metal, concrete,(Funk et al., 2019) or wood,(Pantano et al., 2018; Clar et al., 2019; Platten et al., 2016) have been studied. Specific concerns about the release during food contact were excellently reviewed by the Franz group,(Störmer et al., 2017; Franz et al., 2020) and by the Duncan group.(Duncan and Pillai, 2014) In short, diffusion of nanomaterials inside polymers is far too slow to allow migration into food, but degradation and dissolution of either matrix or nanomaterial can induce releases. In this regard it is astonishing that paper-based packaging has not received more attention, since these conditions of suppressed migration may not apply. The research gap is all the more astonishing since the paper industry is an important sector (400 million tons per year) that consumes 32 million metric tons of inorganic fillers per year.(Hubbe and Gill, 2016)

Although packaging based on paper or cardboard would be intended for dry food only, consumers recycle paper-based materials, and one cannot entirely exclude the unintended contact of other foodstuff to paper and its fillers. Also, for mechanistic understanding of the main factors that determine releases in food contact, the comparison between different polymer-NEPs and paper-NEPs is promising. In polymers, dyes or pigments provide color, but dyes, being molecularly dissolved in the polymer, have a higher potential to migrate than pigments, which are nano- or micro-particles that are simply too big to migrate.(Störmer et al., 2017; Bott et al., 2014) A critical review has been devoted to the issue with specific attention to NEPs with embedded Ag, where the manifold reaction pathways of Ag + ions to reprecipitate into particles after release represents a particular conceptual challenge.(Jokar et al., 2017) Many studies focused on the highest priority matrix (polyolefines, especially polyethylene) thus there is little information about the systematic trends for other polymers.(Störmer et al., 2017; Franz et al., 2020) In and on paper, calcium carbonate, kaolin and other clays, talc, silica, and various pigments serve different purposes. Some of the relevant grades are now identified as nanomaterials. Silica is added to cellulosic fiber slurries before paper formation, influencing structure, appearance, and final properties of finished products. In addition, silica accelerates the rate of drying during manufacturing (less energy needed) and reduces cellulose consumption (replaced by fillers). Kaolins reduce ink penetration and enable sharp prints. Other fillers modulate the brightness and opacity of paper.

The global market of nano-enabled packaging for food and beverages is predicted to grow rapidly in the coming years. The size of the market was valued at US\$ 30.6 billion in 2017 and in 10 year is expected to triple its value (USD 89 billion in 2026).(Nano-Enabled Packaging Market Share, Size, Trends, 2019) Marketing surveys often only count products with unique and novel properties, whereas the European REACH definition of a nanomaterial has a wider scope and identifies a majority of the total production of some materials, specifically of SiO₂ and of some pigments, as nanomaterials,(Wigger et al., 2018) and demands registration and evaluation of each of their different “nanofoms” (NF).(Commission, E, 2018) The actual market size of FCMs that

incorporate NFs may thus be even larger.

NFs are described by size, shape, crystallinity, surface area and surface treatment.(European Chemicals Agency (ECHA), 2019) This distinction creates transparency on different grades that have been developed and commercialised to optimize the performance for different needs and applications. For example, some grades may be more suitable for the inclusion in food contact NEPs than others. It is only fair to ask to what extent the release in food contact differs between NEPs using different NFs, or different matrices. For hazard assessment, grouping of NFs is relatively well established.(Commission, E, 2018; European Chemical Agency (ECHA), 2019) No one has yet proposed a grouping of NEPs, since regulation addresses the FCM *ingredients*, some of which may be NFs, but not the final NEP. But also the scientific prerequisites are missing: One first needs to achieve a ranking of the relevance of nanoform descriptors, matrix identity, and food simulant choices.

Here we compare the release behavior of different NEPs by systematically varying diverse factors: a) NF substance (SiO₂, Fe₂O₃, CaCO₃, CuPhthalocyanine), b) NFs characteristics (size, crystallinity, surface), c) NF load (few ppm to 2.3%), d) host matrix (paper, polylactic acid, polyamide, polyurethane, polypropylene, coated wood), e) food simulants (3% Acetic acid, 10% Ethanol, nanopure water) and f) kinetics (up to 14 days). We benchmark our methods against a previously tested (Pillai et al., 2016) representative material donated by the US-FDA. By comparative testing in the above multidimensional parameter space, we obtain the x-fold similarity(Jeliaskova et al., 2021; Jeliaskova, 2021) between different NEPs and different test conditions. This results in a ranking of the relevance of nanoform descriptors, matrix identity, and food simulant. Ultimately, our work shall simplify the early assessment of the safe use of FCMs via concepts of analogy and similarity, where parameters and descriptors of the NEP matrix and intended use may be more important than the NF descriptors, which are the basis of current regulation.

2. Materials and methods

2.1. Paper, plastic NEPs and the related fillers characteristics

This study focuses on the release in food simulants of various nanoparticles and nanofoms embedded in different matrices. Three matrices were used: paper, polymer, and paint (on wood). The paper matrix of cellulose contained two different types of nanomaterials, anisotropic silica and iron oxide, each with two nanofoms (Table 1). Similarly, the polymer matrix was studied with three different types of polymers, Polylactic Acid (PLA), Polyamide (PA6), and Polyurethane (PU), one nanomaterial, the pigment Cu-Phthalocyanine, with two nanofoms (Table 1). In addition, polypropylene (PP) was used with an iron oxide filler. Lastly, an acrylic wood coating with the same iron oxide nanomaterial was also tested.

The tests were guided by the European Regulation EC 1935/2004 and EU 10/2011 tested at 40 °C with three different food simulant fluids: 10%(v/v) Ethanol (EtOH), 3%(v/v) Acetic acid (AcOH), and nanopure (NP) water.

The regulation EU 10/2011 suggests exposure for 10 days at 40 °C when testing food plastic contact materials. Our method complies with the regulation by using the standardised temperature and food simulation fluids, with sampling time points at 2 h, 24 h, 72 h, 168 h, 240 (= 10 days) and 336 h. The 14 day sampling time point was added to examine potential saturation of release rates past the ten days. In addition, an exposure study with 3 days at 40 °C was performed on paper with 85 g/m². There are no applicable regulations since the paper goods regulation examines thicker paper goods such as cardboard. All food simulant fluids used Milli-Q purified water.

2.2. Sample preparation and testing

Two different types of nanomaterials were used for the cellulose

Table 1
Food contact study overview.

Nanoform	Size of NF by TEM (nm)	Shape of NF	Conc. of NF in NEP (% w/w)	Matrix	Food simulant ^a	Study condition ^a
Si_anis_std	7	Elongated	0.5, 0.3, 0.01, 0.006	Cellulose with CaCO ₃	A, B, w	3 days at 40 °C
Si_anis_Al	7	Elongated				
Fe ₂ O ₃ _nano_A	9	Elongated	0.5, 0.005	Cellulose with Si_anis_Al (0.05% w/w) and CaCO ₃	A, B, w	3 days at 40 °C
Fe ₂ O ₃ _nano_B	43	Spheroidal				
CuPhthalo_α	17	Spheroidal	1	PLA, PA, PU	A, B	14 days at 40 °C
CuPhthalo_β	14	Spheroidal				
Fe ₂ O ₃ _nano_B	43	Spheroidal	2.3	Paint	B	3 days at 40 °C
Fe ₂ O ₃ _nano_B	43	Spheroidal	1	PP	B	3 days at 40 °C

^a Food simulant and study conditions: *Food simulants* A: 10%(v/v) Ethanol, B: 3%(v/v) Acetic Acid, w: nanopure water. *Study conditions*: 3 days at 40 °C; 14 days at 40 °C (Sampling at 2 h, 1-day, 3-day, 7-day, 10-day, and 14-day).

paper studies. A cellulose matrix filled with the conventional (non-nano) form of calcium carbonate was used to reach 25% remaining mass after ashing. The two types of nanomaterial used were anisotropic amorphous silica (SiO₂_anis, provided by Nouryon) and iron oxide (Fe₂O₃, provided by BASF SE). The anisotropic silica had two variations, silica with aluminum and standard silica, both amorphous. The two variations were tested at various loading concentrations (Table 1). The second nanomaterial, iron oxide also was tested in two variations, nano_A and nano_B at high (0.5% w/w) and low (0.005% w/w) loading concentrations. Fig. 1 demonstrates that different NFs of the same substance achieve different color perception, and thus enable the variety of colored consumer products (Table S2).

All paper samples had an exposed diameter of 38 mm and the papers were all cut using a 45 mm punch hole. The piece of paper was then placed inside a custom-made ring (Fig. S1) for the study. The ring was used so that only one side of the paper matrix had full contact with the solvent. In addition, it allowed control of migration from within the matrix and prevented migration from the cut edge. Each piece of paper was weighed prior to it being placed in the ring which allowed for the analysis to be done on a per mass basis. Once placed in the ring, the paper sample went into a 300 mL LDPE container and 10 mL of solvent was added.

After the addition of solvent, each sample was checked for air bubbles. Air bubbles were removed through side slits at which point the samples could be placed in an oven (Memmert GmbH) at 40 °C. For all studies two controls were used: 1) solvent only, and 2) an empty ring with solvent. The controls provided a background value for the desired elements which the paper samples could be compared against. The paper studies lasted 3 days at 40 °C; once the time had lapsed the sample solution was placed in storage vials and the paper was air dried in a fume hood. A 100 µL sample was taken from the storage vial stabilized with

1% (v/v) Nitric Acid (HNO₃) solution for a 1:100 dilution ratio and analyzed with ICP-MS (Perkin-Elmer NexION 2000) for Fe, Si, and Ca. The dried paper was sputtered with 10 nm of carbon and prepared for SEM-EDX analysis (ThermoFisher Scientific Phenom).

BASF SE provided the three different polymers studied, PLA, PA6, and PU, as well as Cu-Phthalocyanine. The polymers represented a range of polymers which contain different chemical, thermal and mechanical properties (Table S1) and allowed to see the resiliency of the matrix when exposed for 14 days at 40 °C. All polymers were of thermoplastic grade with molar masses above 40 kDa. The polymer matrix was exposed for a longer period than the paper matrix as it is more resilient. Two nanoforms of Cu-Phthalocyanine with same chemical composition but different crystallinity were considered: Cu-Phthalocyanine_nano_α and Cu-Phthalocyanine_nano_β, known as Pigment Blue 15:1 and 15:2 respectively. The pigment was embedded in the polymer at a concentration of 1%(v/v). Fig. 1 demonstrates a) that this concentrations induces deep blue color, and is thus representative of realistic conditions, and b) that different NFs also of this same substance achieve different color perception (Table S2). Due to the pigments high hydrophobicity these studies were tested without nanopure water and instead they were tested with two food simulant fluids: 10% (v/v) EtOH and 3% (v/v) AcOH.

The sample size tested for the three polymers was 5 cm × 5 cm × 0.5 cm and was fully submersed in 50 mL of the food simulant for testing (Fig. S2). The samples were all weighed before the study and placed in LDPE containers. A set of controls was used for all three polymers in which a set of samples (triplicate) were studied without the pigment (polymer only) in both food simulant fluids. Once placed in the oven, 0.5 mL sampling of the solution was obtained at 2-h, 1-day, 3-day, 7-day, 10-day, and finally at 14-day. Each of the solutions taken was stabilized with 1% (v/v) HNO₃ at a dilution ratio of 1:20 and analyzed with ICP-MS for Cu.

The Fe₂O₃ nanoforms were finally tested when embedded as pigments in wood paint. The acrylic polymer matrix of the paint was provided and applied by Nouryon and it contained pigment at a concentration of 2.3% (w/w). The paint was applied only to one side (8 cm × 8 cm) of wood plate. Fig. 1 demonstrates as for the other cases that this concentration induces deep red color, and is thus representative of realistic products, and that again different NFs of the same substance achieve different color perception, as intended (Table S2).

2.3. Analysis

2.3.1. Colorimetry

Pigments such as Fe₂O₃ and Cu-Phthalocyanine are embedded in plastics or paper *with the intention* to provide color. Colorimetric evaluations were done according to the spectral method described in ISO 18314-1 (2015) with d8° geometry. Resulting color coordinates ΔL*, Δa*, Δb*, ΔH*, ΔC*, and ΔE* (Fig. S3) were evaluated in accordance with ISO 11664-4 (2008) for light source D65 and 10° standard observer from the measurements over a white substrate. Detailed results are

NF comparison	Matrix	NF % w/w	ΔE*
Fe ₂ O ₃ _nano_B Fe ₂ O ₃ _nano_A	Paper	0.5	4.4
		0.05	2.5
		0.005	0.7
CuPhthlo_nano (α) CuPhthlo_nano (β)	PA6	1	6.4
	PU	1	4.5
	PLA	1	8.7
Fe ₂ O ₃ _nano_B Fe ₂ O ₃ _nano_A	paint	2.3	41.2
	formulation	0.33	6.8

Fig. 1. Comparative colorimetry analysis: The difference in color coordinate ΔE* (total distance in the CIELAB color space, ISO 11664-4) is calculated for different NFs of the same substance. Fe₂O₃_nano_B vs. Fe₂O₃_nano_A are different particle sizes. The color indices of Pigment Blue 15:1 and 15:2 respectively designate the α and β crystalline forms of CuPhthalocyanine, and again result in measurable differences of the colorimetric appearance, as intended. (For interpretation of the references to color in this figure legend, the reader is referred to the web version of this article.)

reported in the SI (Table S2). In short, the parameter ΔE^* represents that total difference between two colors, and is in general visually noted by humans when ΔE^* exceeds a value of 1.

2.3.2. ICP-MS and single-particle ICPMS

A Perkin-Elmer NexION 2000 was used for elemental analysis of Si, Ca, Fe and Cu in the food simulant fluids. All samples were stabilized with 1% (v/v) HNO_3 and were diluted to ensure that the samples did not exceed detection limits of the instrument (see section above for dilution ratios). We measured with kinetic energy discrimination (KED) with Helium gas, and ran ^{45}Sc as internal standard. Calibration curves for each analyte was used and verified during each run to obtain concentration values. Al and Fe had a limit of detection (LoD) of 0.1 $\mu\text{g/L}$ with an external calibration of 0.1/1/10/100/1000 $\mu\text{g/L}$ (ppb). For Si, the LoD was 1 $\mu\text{g/L}$ with an external calibration of 1/10/100/1000 $\mu\text{g/L}$ (ppb) in KED mode. The integration time was 50 ms and the argon flow of the Meinhardt nebulizer was 0.92 L/min. In single-particle operation mode, the Perkin-Elmer NexION 2000 was calibrated on an ionic ^{63}Cu standard with a calibration of the particle transfer efficiency on 30 nm and 60 nm Au particles. The dwell time was set to 50 μs .

2.3.3. SEM-EDX

The distribution of the paper fillers before food contact was assessed by EDX of cross-sections at 10 kV with 1.2 nA current and the ESB detector (WD 6.3 mm) for an accumulation time of 300 s and 500 \times magnification. Samples from the treated paper were cut and placed on the holders with the treated side facing up. Silver adhesive was placed on the edges of the paper samples before the samples were sputtered with 10 nm of Carbon (Safematic CCU-010 LV, Labtech). Once ready, the samples were imaged and analyzed (ThermoFisher Scientific Phenom) at a magnification of 1000. Elemental Analysis was done for each sample at the same magnification.

2.3.4. Filtration

To evaluate the form of element release from NEPs, select solutions were filtered after food contact tests. Hydrosart® sartorius membranes were selected with a cutoff of 10 KD. Such cutoff blocks any possible nanoform analyzed in this work, since membrane pores have a size of ca. 3 nm. After filtration, the samples were stabilized with 1% (v/v) HNO_3 , diluted at a 1:10 ratio and analyzed with ICP-MS.

2.3.5. UV-vis spectrometry

The UV-Vis instrument Agilent Cary 5000 is used with 50 mm quartz cells to optimize detection down to 0.005 absorbance units. Calibration of the extinction at peak pigment wavelength for quantification of the dissolved material was performed by dissolving the pigment in concentrated sulfuric acid to get the mass attenuation coefficient of the CuPhthalocyanine pigment of 432 L/(g \cdot cm) at 791 nm. The limit of quantification is found at 2.31 $\mu\text{g/L}$.

2.3.6. Comparison on representative NEP

As a methodical cross-check, we re-analyzed a quantum-dot-containing polymer that had previously been analyzed by Pillai et al., and we obtained consistent results (Table S3, Fig. S4). The quantity of release was assessed on three elements, Zn, Cd, and Se, using two of the same standardised simulant fluids that were reported also by Pillai et al. (Pillai et al., 2016) Only on Cd, we observed systematically less release by about a factor 4, but we confirm the order of magnitude of few ng/cm 2 , and we observed the same sensitivity to acetic acid as reported by Pillai et al. (Table S3). On Zn and Se, our results agree quantitatively within two standard deviations, without a systematic trend (Fig. S4). Remaining differences may also be due to different incubation geometries and to the reproduction of this NEP as new batch of the same recipe (at US-FDA). The uncertainty in the correctness of our measurements is thus estimated at about a factor 2 in the concentration range of 100 ng/cm 2 that is relevant for our case studies.

2.4. Similarity assessment by x-fold algorithm

Methods to quantify pairwise similarity specifically for NFs were introduced and discussed by Jeliaskova et al. (Jeliaskova et al., 2021) In short, the x-fold comparison divides the larger of two values by the smaller, and thus always generates an answer larger than one. Identical NFs measured by perfectly accurate methods would score 1 in this algorithm. It is most appropriate to descriptors that follow log-normal distributions, and which thus cover several orders of magnitude – such as release rates. This model is the basis for many of the criteria of the ECETOC NanoApp[15], is integrated in the GRACIOUS browser-based similarity tool (Jeliaskova, 2021) and in the free GRACIOUS software blueprint. (Traas and Vanhauten, 2021)

3. Results

The results presented here are for three different matrices with nanomaterials exposed to food simulant fluids. We assessed both quality and quantity of releases.

3.1. Silica and iron oxide nanomaterials in cellulose matrix

We first assessed the homogeneity of the fillers across the cross-section of the paper (Fig. S5). The elemental maps for the elements C, O, Ca, Fe, Si, Al demonstrate embedded NFs inside the NEP with slight aggregation of Si and potentially a slight accumulation of Al on one side, but nothing comparable to the layered structures of Kaolin and CaCO_3 gloss coatings on cardboard that were studied earlier. (Zhang et al., 2020) In this case silica is together with cationic polyacrylamide used as a two component flocculation system to improve retention and dewatering. The main part of the Al is added as polyaluminium chloride to enhance the effect of starch as a strengthening agent. The high dosages of silica (0.3 and 0.5% w/w) are very high and are normally not used in commercial papers. The elemental map of Ca demonstrated good homogeneity across the depth and length of the paper. One concludes that CaCO_3 serves here as bulk filler to reduce the cellulose consumption, but not a surface coating to increase gloss. On the paper colored by iron oxides with the concentration needed for the intended coloring (Fig. 1), Fe was only occasionally detectable (Fig. S6); Si and Ca were distributed analogously to the other type of paper (Fig. S5).

Fig. 2 shows the results for the silicon and calcium release from the anisotropic silica paper in $\mu\text{g/cm}^2$ after 3 days in the oven at 40 $^\circ\text{C}$. The values represented in the figure are the averaged values from triplicates after the blank and negative control value were subtracted from the measured value. The error bars represent standard deviation in the samples. These results illustrate that the samples, regardless of the loading concentration and nanoform type, released between 0.5 and 3 $\mu\text{g/cm}^2$ of Si. In addition, calcium values were about 1000 $\mu\text{g/cm}^2$ for all samples treated with 3% (v/v) AcOH regardless of nanoform indicating that the calcium carbonate filler reacts with the acid to CO_2 and calcium ions, which are then leaching out. The images taken from the samples pre- and post-immersion support the claim (Fig. 3). By incubating the calcium carbonate directly in 3% (v/v) AcOH we confirmed its complete reaction to ions.

While the Si release was in the same magnitude there were some differences in release based on food simulant fluid used. For example, Si release from the sample with highest loading of 0.5% w/w immersed in 3% (v/v) AcOH was approximately 3 $\mu\text{g/cm}^2$ versus the 0.5 $\mu\text{g/cm}^2$ released when immersed in NP water. With respect to the loading concentration, the fraction of release were not significantly different: The loading concentration varied by about a magnitude just as the release amount of Si. The difference with food simulant fluid is seen in the Ca released as well, with the samples immersed in 3% (v/v) AcOH releasing almost 1000 $\mu\text{g/cm}^2$ versus the estimated 10 $\mu\text{g/cm}^2$ released when immersed in NP water or 10% (v/v) EtOH. This illustrates the significance of pH on the release amount of Si and Ca in the paper.

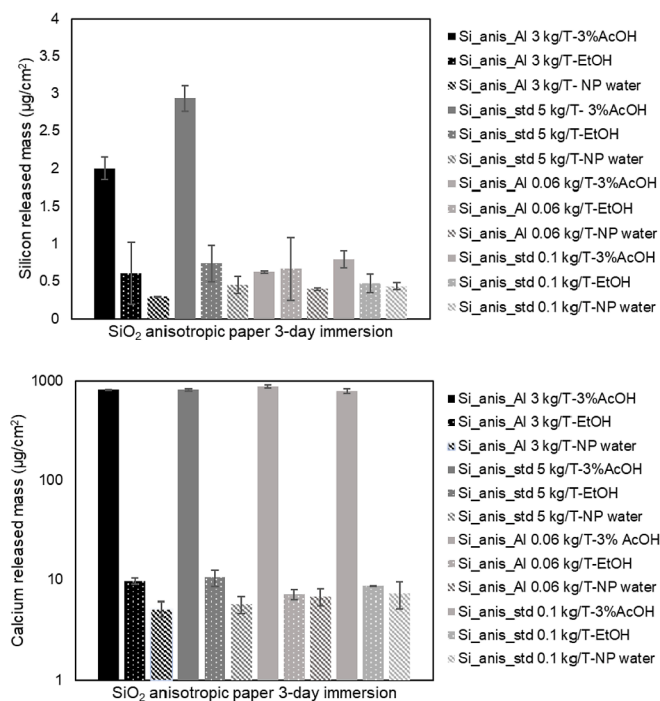


Fig. 2. Si and Ca released mass ($\mu\text{g}/\text{cm}^2$) for both nanoforms of silica in paper (i.e. cellulose matrix) with silica loading from 0.006 to 0.5%w/w. The values represent average values from triplicates and error bars are standard deviations.

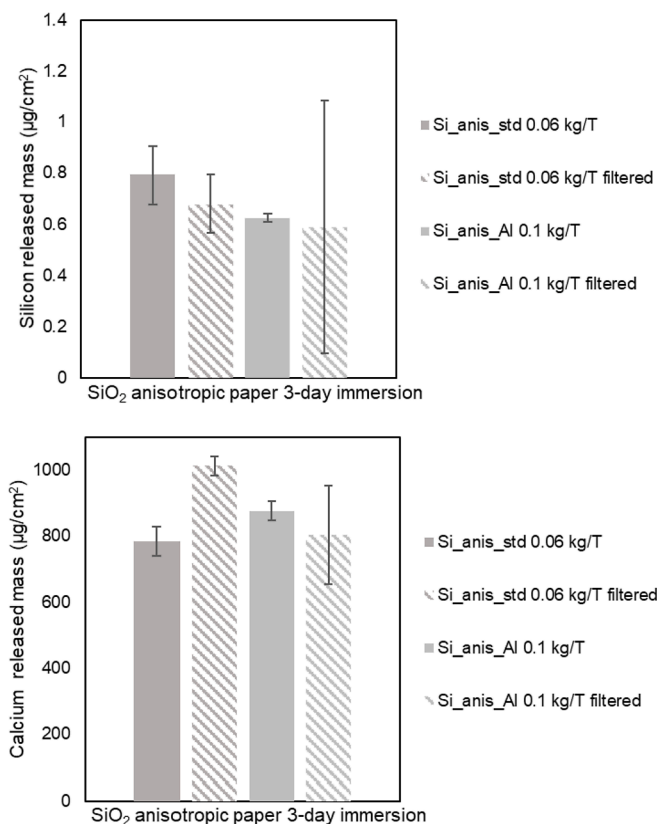


Fig. 4. Si and Ca released mass ($\mu\text{g}/\text{cm}^2$) for filtered and unfiltered paper samples in 3% (v/v) AcOH. Values show average values with error bars representing standard deviations.

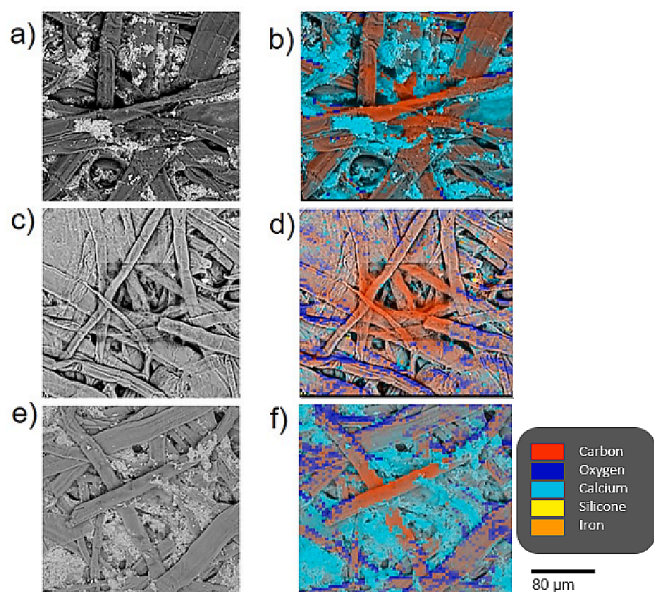


Fig. 3. SEM-EDX images of silica filled papers: a,b) pre immersion; c,d) post immersion in 3%AcOH; e,f) post immersion in deionized water. The magnification is of $1000\times$. Panels on the left (a,c,e) are in SEM mode. Panels on the right (b,d,f) are EDX scans to highlight the elemental distribution.

In Fig. 4, the filtered samples demonstrate that most of the release from the anisotropic silica paper samples was in ionic form since the range of values are within 15% of each other. Previous studies investigating the release from NEPs, e.g. those on Ag releases, (Jokar et al., 2017) or on CuPhthalocyanine and Kaolin, (Zhang et al., 2020) used the highly sensitive technique of single-particle-ICPMS to differentiate between ions and particles, but the small size of the silica particles below 10 nm is below the detection limit of single-particle-ICPMS, at least for

our commercial instrument. We performed single-particle-ICPMS measurements only for the Cu release from plastics (see next section), not for the Si assessment, because it would have remained inconclusive anyway.

Like the anisotropic silica paper, the iron oxide filled paper (Fig. 5) values have blanks and controls subtracted from the measured value. The results show that both the Si and Fe released is in the same unit range, however, in all Fe samples the release stayed below $0.25 \mu\text{g}/\text{cm}^2$ while Si reached a few $\mu\text{g}/\text{cm}^2$. For the Ca released mass there is no large difference in values as the 3% (v/v) AcOH immersed samples are about $1000 \mu\text{g}/\text{cm}^2$ and the rest are close to and below $10 \mu\text{g}/\text{cm}^2$. Unlike the Si release in the anisotropic paper samples the amounts of Fe released from the Fe_2O_3 papers did not exceed $0.30 \mu\text{g}/\text{cm}^2$ and thus the amount of release for this paper is low especially when we consider EtOH and NP water immersion.

The nanoform or loading concentration were not a significant factor in the amount of released mass, as seen by the similar amounts of Fe released for the nano A and B forms of Fe_2O_3 . The largest difference in released mass based on nanoform was seen in the low load concentration of 0.005% w/w, where Nano_B released higher mass than nano_A with the same load concentration, yet, it was only found when the papers were immersed in 3% (v/v) AcOH.

In agreement with the silica paper, the food simulant fluid used is a dominant factor in release concentration. For example, there is approximately $0.02 \mu\text{g}/\text{cm}^2$ and $0.15 \mu\text{g}/\text{cm}^2$ of Fe released for the Fe_2O_3 .B 0.5% w/w sample in water and 3% (v/v) AcOH, respectively. The influence of food simulant fluid is highly seen in the Ca element release, as like the SiO_2 anisotropic paper, where there is a 3-order magnitude difference between the water and 3% (v/v) AcOH immersion samples. Thus, the paper samples nano release show to have a significant dependence on pH of food simulant fluid.

The SEM-EDX images (Fig. 6) are for pre- and post-immersed samples with 10 nm of carbon sputtering. The images are taken at a

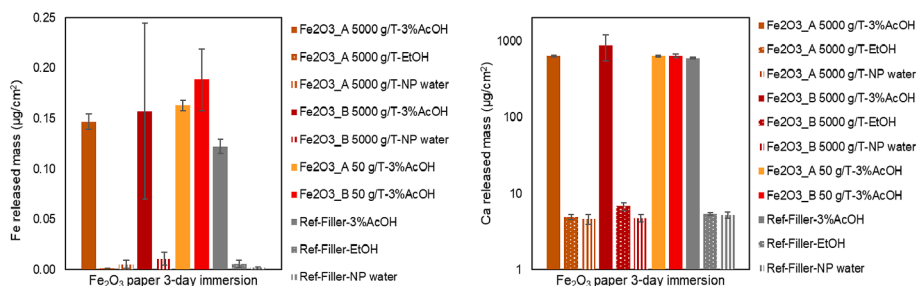


Fig. 5. Fe and Ca released mass ($\mu\text{g}/\text{cm}^2$) for both nanoforms and loading concentrations of Fe_2O_3 (0.5%w/w, 0.005%w/w) in paper (cellulose matrix). Ref-Filler indicates a reference paper with a commercially typical filler content. Values represent averaged values with error bars as standard deviations.

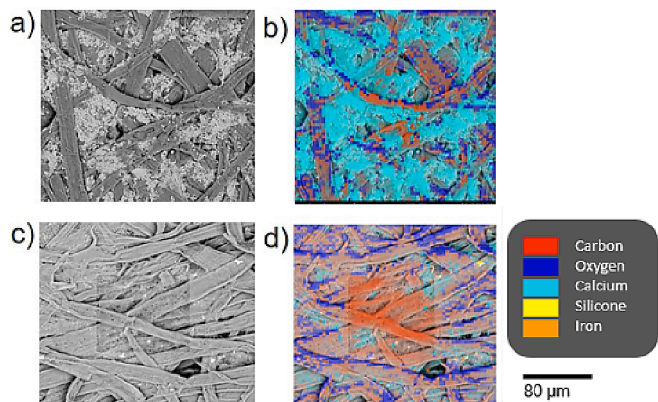


Fig. 6. SEM-EDX images of iron oxide filled papers a,b) pre immersion; c,d) post immersion in 3% (v/v) AcOH. The magnification is of 1000 \times . Panels on the left (a,c) are in SEM mode. Panels on the right (b,d) are EDX scans to highlight the elemental distribution.

magnification of 1000 and are in the μm scale. The images illustrate the structural differences of the paper under different conditions. The large amount of Ca release when the papers are immersed in 3% (v/v) AcOH can be seen as the calcium carbonate clusters are missing, thus, conforming the large values of Ca release measured by ICP-MS.

Since the images in Figs. 3 and 6 were obtained in the μm scale, the nanomaterials consisting of Si and Al cannot be readily seen or measured thus EDX measurements cannot be used to quantify differences of the elements pre- and post-immersion. However, since the samples immersed in the 3% (v/v) AcOH lost much of its calcium carbonate, the ensuing EDX analysis in Fig. 6d was able to measure more Si and Al than the pre-immersed samples in Fig. 6b. This confirms that the releases induced with the 3% (v/v) AcOH remain incomplete, since fillers remained in the paper.

There was not much of a visual difference of the cellulose matrix seen in the SEM images across the different immersion conditions. The cellulose matrix was not found to be highly impacted by the treatment. For the case of the 3% (v/v) AcOH there is some thinning and shrinking of the cellulose strands, but the strands are delineated and spread across the imaged area as seen in the rest of the images. Therefore, the amount of cellulose matrix disintegration that may occur in a 3-day study remains inconclusive.

Overall, both the ICP and SEM-EDX data shows that while different nanoforms, loading concentrations, and substances were used the released mass were similar. The released mass in all cases stayed in the $\mu\text{g}/\text{cm}^2$ range and had similar release mass with each food simulant fluid indicating that matrix resiliency and characteristics as well as food simulant fluid (i.e. food contact application) were more significant factors in the release.

3.2. Copper-containing pigments in plastic polymer matrix (PU, PLA, and PA)

For Cu-Phthalocyanine pigment in plastic, an earlier study used TEM and single-particle-ICPMS to assess the form of release, finding no particles, only ions. (Zhang et al., 2020) That study used one specific NF of Cu-Phthalocyanine, which had the α crystallinity, in one specific polymer, which was the very hydrophobic polypropylene. Here we are building on this earlier finding and compare the quantitative similarity of release rates by detecting Cu release from NEPs with different polymer matrices and NFs of different crystallinity and impurity. The Cu-Phthalocyanine pigment is almost insoluble also under acidic conditions, because the Cu is complexed in the Phthalocyanine ring, but the industrial material contains trace impurities of unbound Cu from the synthesis process. Fig. 7 shows the results for Cu released from 14-day immersion studies in three different plastic polymer matrixes. The values from all released mass results were in ng/cm^2 , a magnitude smaller than that seen for the release values of Si and Fe in paper. Thus, these results show that the plastic polymer matrixes are more resilient to fluid penetration.

For all plastic polymer matrixes, as immersion time increased so did amount released of Cu. This observation held for all food simulant fluids tested. For example, in PU samples, the measured amount of Cu increased in the β form from approximately $5 \text{ ng}/\text{cm}^2$ to $40 \text{ ng}/\text{cm}^2$ in 334-h of immersion in 3% (v/v) AcOH.

The increase release rate did vary by polymer matrix regardless of food simulant fluid used with PLA releasing the least amount of Cu and PU releasing the most amount of Cu (Fig. 7a). It is speculated that the effect from the matrix is due to the water uptake and glass transition temperature of the plastic polymer. TPU has the lowest glass transition temperature from the three polymers (Table SI 1), thus probably higher molecular mobility, whereas PA has the highest water uptake of up to 12%. Therefore in the release from PA and PU is influenced by the mobility of ions and solvent inside the matrix. Therefore, each of the polymers tested showed varying matrix resilience.

Not only did the plastic polymer matrix have an influence on Cu release, there is also an NF influence on the release in one case (Fig. 7b). When the PA polymer samples were immersed in 3% (v/v) AcOH, the β form released over 2-fold more Cu than the α form, but also differed in the release kinetics (Fig. 7b). This difference is observed only for the PA polymer matrix and not observed for the PU samples, which have a higher background from the pigment-free polymer (Fig. 7c). The PU samples (Fig. 7c) demonstrates that the NEPs containing the α and β NFs release similar amounts of Cu.

On PU, the food simulant fluid influence is limited: the PU samples immersed in 3% (v/v) AcOH release from 1.5-fold to 3-fold more Cu than the PU samples immersed in 10% (v/v) EtOH (Fig. 7c). This difference between food simulant fluids is much more pronounced on PA with up to 30-fold difference (Fig. 7b).

Thus, similarly to the paper samples, the polymer samples follow a trend, where the released mass varies by food contact application. However, it also indicates the importance of matrix resiliency and

a)

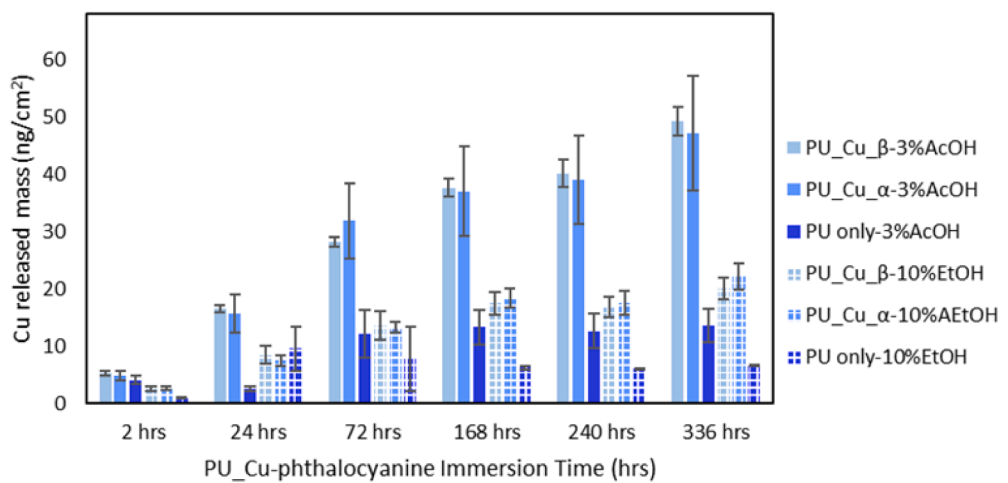
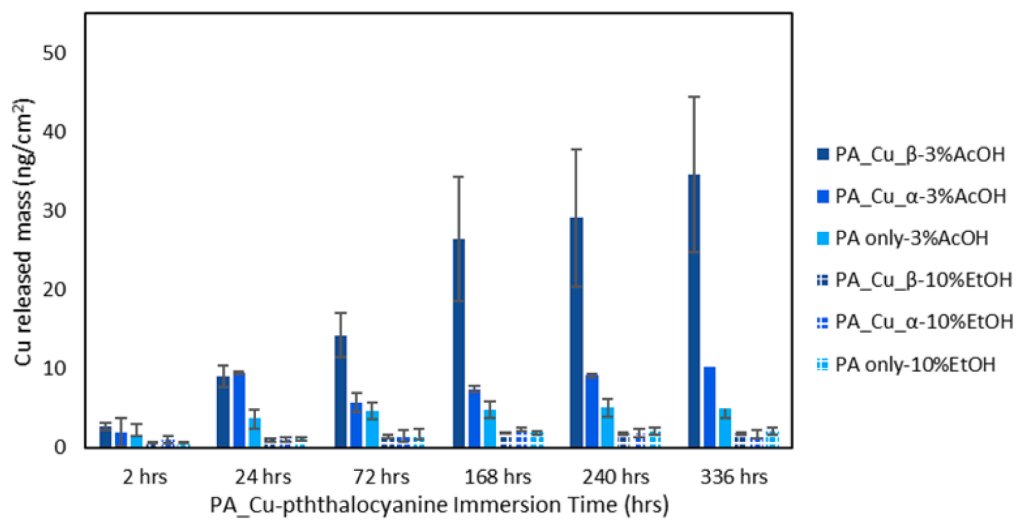
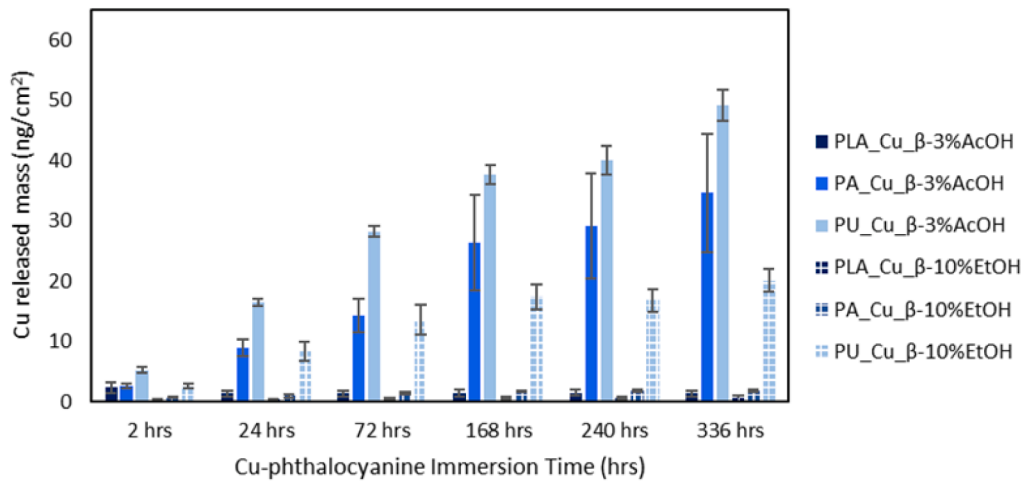


Fig. 7. Cu released mass (ng/cm²) over time for PLA, PA and PU polymer matrices for all three sample types and food simulant fluid. Values represent an average of three measurements with standard deviation shown as the error bar.

medium penetration. Even after the 14 day period, the total released 2.5 μg Cu represented only a marginal fraction, specifically $2.08 \cdot 10^{-5}$ of the 0.12 g Cu that are contained in the pigments which are contained in the polymer. Additionally, the reduction of time-dependent release rates between day 0 and day 3 (Fig. S7) supports the assumption that the release occurs from the surface or near surface layers. The rate decrease over time is very similar in both solvents thus it may be an indication of the transport mechanism in which the medium diffuses with the ions out of the polymer, as investigated earlier on PP composites. (Jablonski et al., 2019)

3.3. Release of Cu is not evidence of the migration of pigment

In Fig. 8 it is seen that the form in which the Cu is released is ionic just as the Fe and Si, since the filtered and non-filtered samples result in similar values of Cu especially for the PA samples (Fig. 8c). If the release were another type (i.e. particulate) then the filtered samples would show a significant reduction of the Cu released mass. The measured increase of filtered values for the PU samples is not statistically significant. Additionally, single-particle ICPMS confirmed the higher ionic Cu background in leachates from the PA with the β form (Fig. 8b) than in leachates from PA with the α form (Fig. 8a), but in both cases, the single-particle ICPMS found no Cu-containing particles. This finding is consistent with extensive single-particle ICPMS and TEM analyses on the releases from Polypropylene (PP) containing CuPhthalocyanine, which were tested for food contact via immersion in 3% (v/v) AcOH and 10% (v/v) EtOH at 40 °C, finding no particle releases. (Zhang et al., 2020) Finally, we performed UVVis spectrometry to assess the released amount via the characteristic absorption of Phthalocyanine. All spectra remained below the limit of quantification at 2.31 $\mu\text{g}/\text{L}$, thus confirming the absence of particle release. One may argue that the Cu could originate from protonation of the pyrrolic nitrogens, thus liberating coordinated metals and generating free base forms of the phthalocyanine. This hypothesis does not explain the difference between crystalline forms, but anyway it was tested by incubating the Cu-phthalocyanine at 10 mg/L directly in the 3% (v/v) AcOH at 40 °C, without any polymer matrix. After 14 days incubation and filtration, only 0.049 mg/L of Cu were found. That trace level of soluble Cu rejects the hypothesis of liberation of Cu from the Cu-Phthalocyanine, but matches the hypothesis of a soluble impurity. Taken together, the one case of a difference between NFs (PA with either CuPhthalocyanine in α form or in β form) is clearly attributed to leaching of a Cu-containing impurity, and not the differences in the behavior of the actual particles.

3.4. Case study: varying the matrix on iron oxide filler – paint on wood, paper, and plastic

Fig. 9 demonstrates the results of testing iron oxide in three different matrices: paper, paint (on wood), and plastic (polypropylene—PP). The

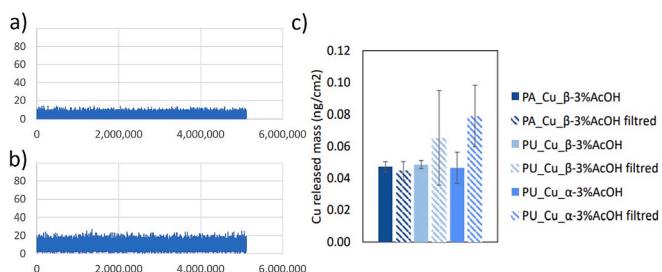


Fig. 8. Testing the particle content among the releases in samples immersed in 3% (v/v) AcOH: single-particle ICPMS of a) PA with CuPhthalocyanine β form, b) PA with CuPhthalocyanine α form. c) total ICPMS on unfiltered and filtered samples. Values represent an average of three measurements with standard deviation shown as the error bar.

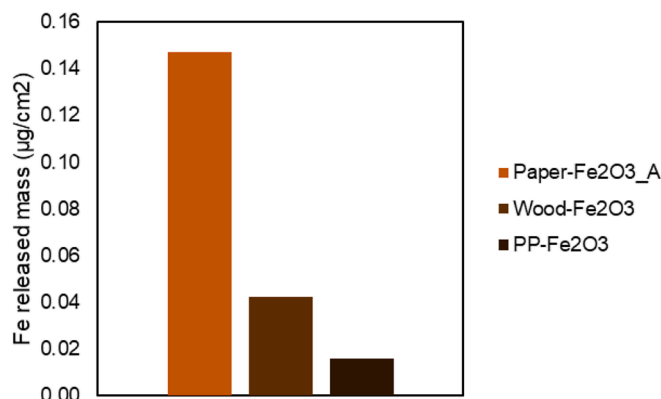


Fig. 9. Fe released mass after immersion in 3% (v/v) AcOH food simulant fluid: from paper (red), from an acrylic coating on wood support (brown), from PP (black). (For interpretation of the references to color in this figure legend, the reader is referred to the web version of this article.)

highest release was measured in paper while the plastic polymer matrix releases the least. Thus, nanoform release may be dominated by matrix type consistent with the rest of results shown in this study. Further analyzing the released mass by filtering solutions of iron oxide nano_B from PP finds no significant difference, illustrating that the release form is ionic (data not shown).

4. Discussion

Regulation, guidance and literature is available on polymer based NEPs for use as food contact material. Regulation EC1935/2004 established general principles for any food contact material, but does not specifically consider nanomaterials. Regulation EC10/2011 does consider nanomaterials as additives in polymers, and authorizes 11 specific cases of polymer, nanomaterial and intended use. There is, however, no general agreement if each NF of the same substance (falling within the specifications of the authorization) requires independent testing. However, if the matrix is specified, the authorization is not valid for another one (this is e.g. the case for TiN). If the matrix is not specified in the authorization, or only a general specification is given, it is authorized under those conditions. The screening tests that we applied focus on ICPMS detection of the total rate of release, and can be interpreted by various algorithms as measure of quantitative similarity. Table 2 chooses the simple x-fold pairwise comparison, which is one of the methods to quantify similarity that is recommended by the white paper on NF similarity. (Jeliazkova et al., 2021) As a methodical cross-check, we re-analyzed a quantum-dot-containing polymer that had previously been analyzed by the US-FDA, and we obtained consistent results (Table S3, Fig. S4). While this material is slightly exotic and not a typical FCM, the use of representative test materials in general is very much advised. Any of our paper and polymer materials could equally serve this purpose in the future.

For the NEPs that we studied, the NFs are embedded homogeneously in a matrix. For this case, the form of release was exclusively ionic. The qualitative similarity of the release from any pair of NEPs is thus high in our case. The test cases that can be compared to assess quantitative similarity are listed in Table 2 and can be summarised as follows:

- the quantitative release changes up to 29-fold by using different food simulants, and changes up to 35-fold by different NEP matrices
- the quantitative release changes up to 1.5-fold by incorporating different NFs (of the same substance) in paper, and up to 3-fold by incorporating different NFs (of the same substance) in plastics.
- Comparing different NF substances in the same penetrable NEP matrix, the total release differs up to 10,000-fold between Fe₂O₃ in paper and CaCO₃ in paper.

Table 2

Summary of the similarity of release rates under variation of each one specific parameter while all others are held constant.

Factor that is varied between cases	Cases	x-fold similarity	Factor ranking
Nanoform characteristics	SiO ₂ vs SiO ₂ -Al (3 media, 1 matrix)	1.47	Low
	CuPC α vs CuPC β (3 media, 3 matrixes)	1.04	
	Fe ₂ O ₃ -A vs Fe ₂ O ₃ -B (3 media, 1 matrix)	1.06	
Nanoform load	SiO ₂ (2 conc., 1 media and 1 matrix)	3.71	No threshold behavior. Total si release scales with nf load
	SiO ₂ -Al (2 conc., 1 media and 1 matrix)	3.20	
	Fe ₂ O ₃ -A (3 conc., 1 media and 1 matrix)	1.11	
	Fe ₂ O ₃ -B (3 conc., 1 media and 1 matrix)	1.19	
	SiO ₂ (3 media and 1 matrix)	6.85	
Food simulant medium	SiO ₂ -Al (3 media and 1 matrix)	6.48	High
	Fe ₂ O ₃ -A (3 media and 1 matrix)	29.40	
	Fe ₂ O ₃ -B (3 media and 1 matrix)	14.27	
	CuPC α (3 media and 3 matrixes)	6.13	
	CuPC β (3 media and 3 matrixes)	20.62	
NEP matrix	CuPC α (1 media and 3 matrixes)	22.11	High
	CuPC β (1 media and 3 matrixes)	34.95	
	Fe ₂ O ₃ -A (1 media and 2 matrixes)	9.19	

One can thus conclude that the main factors that influence the level of NF release are:

- the NEP matrix resilience to food simulant medium. Literature (Störmer et al., 2017; Bott et al., 2014; EFSA Scientific Committee, 2011) and our experiments showed that NFs ($d > 3$ nm) immobilized within an undamaged matrix do not migrate in food simulant medium. In the case of quite severe contact conditions, NEP matrices can undergo a thermo or chemical degradation and release NFs. Schmidt et al. reported the release of Mg-Al double hydroxide platelets from PLA after 10 days at 40 °C in 95% ethanol, which generated the ethanolsis of the polymer. (Schmidt et al., 2011)
- the permeability of NEP matrix to food simulant medium. In line with our experiments, Echegoyen et al. (2016) and Farhoodi et al. (2014), reported the majority of NF release is in ionic forms. (Echegoyen et al., 2016; Farhoodi et al., 2014) Thus, the main NF release originates from their dissolution within the polymer. Increasing food simulant medium absorption in the matrix, NF dissolution is increased as well. NEPs that contain the NF as coating or layer represent a separate class of materials, which can still be assessed by the same rule: Such a composite structure would be considered as “permeable”, because the food (simulant) reaches the NF. One recent report on cardboard with a base coating of CaCO₃ and a top glossy coating of Kaolin and CaCO₃ reported the near-complete release of Ca as dissolved ions in 3% (v/v) AcOH, and a significant release of Al (as tracer of Kaolin)

with occasional release of identified Kaolin platelets. (Zhang et al., 2020)

- the solubility of NF in the food simulant medium. Weiner et al. (2018) and Zhang et al. (2020) underlined the importance of solubility of the NFs in the solvent. (Pillai et al., 2016; Zhang et al., 2020; Weiner et al., 2018) The GRACIOUS case studies found in case of CaCO₃, the Ca-trace release increased by orders of magnitude when in contact with 3% (v/v) AcOH instead of water.
- the size of the NF. Only in case of very small NFs ($d \leq 3$ nm), the migration from the matrix to foodstuff might be possible (Bott et al. 2017 and 2014). (Störmer et al., 2017) One review contested the general validity of the size-controlled migration rules but conceded that “However, the solubility of Ag (particular in an acidic medium) and its tendency to react with chlorine and sulphur to form Ag salts make it a difficult case for studying migration and answering the generic question whether or not ENMs can migrate from FCMS”. (Jokar et al., 2017)

CuPhthalocyanine is a special case, since it is subject to numerous regulations, including regulation (EC) No 1935/2004, Art. 3, Risk Assessment in manufacturer / supplier responsibility, and Commission Regulation (EU) No 10/2011, listing of authorized monomers and additives. Colorants are not listed but may be used in the manufacture of plastic layers in plastic materials and articles subject to national law. No approval from authorities is needed but self-assessment in manufacturer's/supplier's responsibility according to Art. 19 10/2011 and Art.31935/2004, concerning especially the purity requirements on heavy metals, PCB and Carbon Black.

Our findings support the regulatory focus on metallic impurities. Our findings do not provide a basis for additional nano-specific requirements. The one case of a difference from NEPs prepared with different NFs was given by the PA polymer samples immersed in 3% (v/v) AcOH, where the β form released over 2-fold more Cu than the α form, but differed in the release kinetics (Fig. 7b), and neither single-particle-ICPMS nor filtration detected particles, and UV-Vis detected no Phthalocyanine (Fig. 9). All evidence is consistent with the release of a copper impurity. In fact, such impurity was recently confirmed on the pure CuPhthalocyanine pigment: The time course of the copper release in acidic physiological fluids showed an initial copper release in the first two days, which vanished afterwards, and which represented up to 5% of the total Cu content. (Stratmann et al., 2021) The actual particle dissolution rate was below 0.01 ng/cm²/h, consistent with the lack of systemic availability. (Stratmann et al., 2020) Taken together there is no indication of any other release mechanism than the dissolution of a Cu impurity, which can be different between different NFs, but which is not part of the nanoparticle, and which is most accessible in PA due to its high water uptake.

We believe that our ranking of factors controlling the release under food contact conditions can support concepts of analogy during safer-by-design considerations in the research and development of novel food contact materials. For example, for paper and paperboards, many research groups are studying new NFs to further improve mechanical, printability, optical and gas barrier characteristics. Some examples of nanomaterials for future implementations are: nanocellulose (for high biodegradable and sustainable products), nano pigments (for better optical and barrier properties), TiO₂ and SiO₂ (antifungal, deodorizing agents). Improved packaging provides enhanced mechanical, thermal, and barrier properties of the product. (Duncan, 2011; Cerqueira et al., 2018) Such matrices are filled usually with bidimensional NFs (e.g. Kaolin, (Sanchez-Garcia et al., 2008) Montmorillonites, (Chowdhury, 2008; Shi and Gan, 2007) Mica (Chang et al., 2007)) in 5–10% concentrations. Active packaging provides a direct contact between NF and food or food environment to improve product protection. Additionally, NFs with other functionalities (e.g. oxygen scavengers, bio-chemical contamination sensor) are under development and may enter in the

market in close future. The food-packaging industry is assuming their implementation for achieving improved food conservation – but will have to ensure their safe use and regulatory acceptance. In the US, the FDA is the main authority for regulation of food contact materials. The food contact notification process requires industry to provide sufficient scientific information to demonstrate that additives employed are safe for the intended use. The US FDA does not consider NEPs a priori as intrinsically hazardous for human health. Nevertheless, the FDA suggests a case-by-case approach for safety assessing of FC articles. In the EU, Regulation (EC) No 1935/2004 lays down general principles for any food contact material. Specifically for plastics (polymers), the regulation 10/2011 includes a list of authorized substances and additives. The list implicitly includes twelve narrowly specified NEPs (both the additive in nanoform and the polymer matrix are specified). Among the authorized nanoforms are silica and Kaolin, but not calcium carbonate, iron oxide or CuPhthalocyanine. The EU Regulation (EU) No 10/2011 established an overall migration limit (OML), which limits the total quantity of substances migrating into food simulants to $10 \text{ mg/dm}^2 (= 100 \text{ }\mu\text{g/cm}^2)$ per food contact surface area. The releases measured in the present contribution from NEPs containing NFs range between few ng/cm^2 to $1 \text{ }\mu\text{g/cm}^2$ which is still a factor 100 below the OML, and represents dissolution, not migration of the NF. We measured values up to $1000 \text{ }\mu\text{g/cm}^2$ Ca release, but CaCO_3 was not added as a NF but as a conventional (non-nanoform) to the paper, and it is not the intended use of paper to wrap acetic liquid foodstuff.

Since there is an intrinsic difficulty of measuring substance migration in foodstuff, the European Commission suggested a list of five liquid and one solid material to simulate real food in migration testing. Regulation (EU) No 10/2011, requires explicit authorization for nanoforms of substances, which in practice currently means case-by-case authorization. We believe that concepts of analogy can support the safe and sustainable development of materials for food contact, because the ranking of factors in Table 2 directly leads to grouping principles that can enable early conclusions about the release in food contact with limited testing. We would predict that:

- Same NEP matrices, which incorporate different nanoforms ($d > 3 \text{ nm}$) of the identical substance, present the same order of magnitude of release if used for identical FCM applications.
- Different NEPs aimed for identical FCM applications, which incorporate nanoforms with similar dissolution behavior, will present similar release if the matrices show comparable medium resilience and medium permeability.

5. Conclusion

We compared the release behavior of different nano-enabled products (NEPs) by changing a) nanoform (NF) characteristics, b) NF load, c) NEP matrix, and d) food simulants. In this way four conditions were examined:

- high and low concentration of NFs in the same matrix
- different NF of the same NM in the identical matrix
- the same NF in diverse matrices
- diverse food simulant fluids

The case studies add 7 studies on pigments in plastics (3 NF in 4 matrices), 4 studies on paper (2 NFs each of 2 substances) and 2 studies on paints (2 NF). No evidence of particle release was observed in any of our cases: the *qualitative* similarity (the form of release) was high. This finding was obtained on NEPs with embedded NFs, and may not extend to NEPs with NF coatings, as demonstrated by the detectable food contact release of Kaolin coatings on paper. (Zhang et al., 2020) *Quantitative* similarity of releases depended primarily on the NEP matrix. Testing the same NF in paper vs. in polymer, the release from polymer is suppressed by orders of magnitude. We conclude that the penetration of

the simulant fluid into the NEP is the prerequisite of release, as deduced on less penetrable matrices by the Duncan team. (Jablonski et al., 2019; Gray et al., 2018) The solubility of the NF and impurities in the simulant fluid was the second decisive factor, as dissolution inside the NEP is the main mechanism of release. The highest level of release occurs in an acidic environment, where element emission occurs in ionic forms. We thus observed complete removal of CaCO_3 from paper in acidic medium, whereas Fe and Si signals remained in the paper, consistent with the low release rates in ionic form. In our set of 16 NEPs, only one NEP showed a dependence on the REACH NF descriptors (substance, size, shape, surface treatment, crystallinity, impurities), specifically attributed to differences in soluble impurities, whereas for all others the substance of the nanoform was sufficient to predict a similarity of food contact releases, without influences of size, shape, surface treatment, crystallinity.

The ranking of factors enabled a grouping of NEPs regarding similarities of the rate and form of release in food contact. Different NEPs aimed for identical FC applications, which incorporate nanoforms with similar dissolution behavior, will present similar release if the matrices show comparable medium resilience and medium permeability. This concept of analogy is primarily intended to direct the optimisation of cost, performance, safety and sustainability via safer-by-design considerations in the research and development of novel food contact materials. Pending further validation, it may replace regulatory case-by-case assessment by a scientifically supported grouping approach.

Declaration of Competing Interest

The authors declare that they have no known competing financial interests or personal relationships that could have appeared to influence the work reported in this paper.

Acknowledgements

The GRACIOUS project has received funding from the European Union's Horizon 2020 Research and Innovation Programme under grant agreement No. 760840. We sincerely thank Tim Duncan of the US-FDA for providing specimen of Quantum-Dot-polymer films that enabled benchmarking of our methodology. Hubert Rauscher of EC-JRC and Danail Hristozov of GD are gratefully acknowledged for critical pre-submission review. We thank Kai Werle and Svenja Berit Seiffert for performing single-particle-ICPMS analyses, Philipp Müller for supervising electron microscopy, and Elke Schumacher for performing UVVIS analyses.

Appendix A. Supplementary data

Supplementary data to this article can be found online at <https://doi.org/10.1016/j.impact.2021.100372>.

References

- Bott, J., Störmer, A., Franz, R., 2014. A model study into the migration potential of nanoparticles from plastics nanocomposites for food contact. *Food Packag. Shelf Life* 2 (2), 73–80.
- Chapter 1 - Nanotechnology in food packaging: opportunities and challenges. In: Cerqueira, M.A., Vicente, A.A., Pastrana, L.M., Cerqueira, M.A.P.R., Lagaron, J.M., Pastrana Castro, L.M., de Oliveira Soares Vicente, A.A.M. (Eds.), 2018. *Nanomaterials for Food Packaging*. Elsevier, pp. 1–11.
- Chang, J.-H., Mun, M.K., Kim, J.-C., 2007. Synthesis and characterization of poly (butylene terephthalate)/mica nanocomposite fibers via in situ interlayer polymerization. *J. Appl. Polym. Sci.* 106 (2), 1248–1255.
- Chowdhury, S.R., 2008. Some important aspects in designing high molecular weight poly (L-lactic acid)-clay nanocomposites with desired properties. *Polym. Int.* 57 (12), 1326–1332.
- Clar, J.G., Platten, W.E., Baumann, E., Remsen, A., Harmon, S., Rodgers, K., Thomas, T., Matheson, J., Luxton, T.P., 2019. Transformation and release of nanoparticle additives & byproducts from commercially available surface coatings on pressure treated lumber via dermal contact. *Sci. Total Environ.* 694, 133669.
- Commission Regulation (EU) 2018/1881 of 3 December 2018 amending Regulation (EC) No 1907/2006 of the European Parliament and of the Council on the Registration,

- Evaluation, Authorisation and Restriction of Chemicals (REACH) as regards Annexes I, III, VI, VII, VIII, IX, X, XI, and XII to address nanoforms of substances (Text with EEA relevance.). In: Commission, E (Ed.), 2018. C/2018/7942, Commission, E., Ed.
- Duncan, T.V., 2011. Applications of nanotechnology in food packaging and food safety: barrier materials, antimicrobials and sensors. *J. Colloid Interface Sci.* 363 (1), 1–24.
- Duncan, T.V., 2014. Release of engineered Nanomaterials from polymer nanocomposites: the effects of matrix degradation. *ACS Appl. Mater. Interfaces* 7, 20–39.
- Duncan, T.V., Pillai, K., 2014. Release of engineered nanomaterials from polymer nanocomposites: diffusion, dissolution, and desorption. *ACS Appl. Mater. Interfaces* 7, 1–19.
- Echegoyen, Y., Rodríguez, S., Nerín, C., 2016. Nanoclay migration from food packaging materials. *Food Additiv. Contamin. Part A* 33 (3), 530–539.
- EFSA Scientific Committee, 2011. Guidance on the risk assessment of the application of nanoscience and nanotechnologies in the food and feed chain. *EFSA J.* 9 (5), 2140.
- European_Chemical_Agency_(ECHA), 2019. Appendix R.6–1 for nanoforms applicable to the guidance on QSARs and grouping of chemicals. In: ECHA-19-H-15-EN, ECHA, Ed.
- European_Chemical_Agency_(ECHA), 2019. Appendix for nanoforms applicable to the guidance on registration and substance identification. In: ECHA-19-H-14-EN, ECHA, Ed.
- Farhoodi, M., Mousavi, S.M., Sotudeh-Gharebagh, R., Emam-Djomeh, Z., Oromiehie, A., 2014. Migration of aluminum and silicon from PET/clay nanocomposite bottles into acidic food simulant. *Packag. Technol. Sci.* 27 (2), 161–168.
- Franz, R., Bott, J., Störmer, A., 2020. Considerations for and guidance to testing and evaluating migration/release of nanoparticles from polymer based nanocomposites. *Nanomaterials* 10 (6), 1113.
- Froggett, S., Clancy, S., Boverhof, D., Canady, R., 2014. A review and perspective of existing research on the release of nanomaterials from solid nanocomposites. *Part. Fibre Toxicol.* 11 (1), 17.
- Funk, B., Göhler, D., Sachsenhauser, B., Stintz, M., Stahlmecke, B., Johnson, B.A., Wohlleben, W., 2019. Impact of freeze–thaw weathering on integrity, internal structure and particle release from micro-and nanostructured cement composites. *Environ. Sci. Nano* 6 (5), 1443–1456.
- Gray, P.J., Hornick, J.E., Sharma, A., Weiner, R.G., Koontz, J.L., Duncan, T.V., 2018. Influence of different acids on the transport of CdSe quantum dots from polymer nanocomposites to food simulants. *Environ. Sci. Technol.* 52 (16), 9468–9477.
- Harper, S., Wohlleben, W., Doa, M., Nowack, B., Clancy, S., Canady, R., Maynard, A., 2015. Measuring nanomaterial release from carbon nanotube composites: review of the state of the science. *J. Phys. Conf. Ser.* 617 (1), 012026.
- Hubbe, M.A., Gill, R.A., 2016. Fillers for papermaking: a review of their properties, usage practices, and their mechanistic role. *BioResources* 11 (1), 2886–2963.
- Jablonski, J.E., Yu, L., Malik, S., Sharma, A., Bajaj, A., Balasubramaniam, S.L., Bleher, R., Weiner, R.G., Duncan, T.V., 2019. Migration of quaternary ammonium cations from exfoliated clay/low-density polyethylene nanocomposites into Food simulants. *ACS Omega* 4 (8), 13349–13359.
- Jeliakova, N., 2021. **Browser-Based Similarity Analysis by Euclidean and x-fold Algorithms.** <https://search.data.enanomapper.net/projects/gracious/similarity>.
- Jeliakova, N., Bleeker, E., Cross, R.K., Haase, A., Janer, G., Peijnenburg, W., Pink, M., Rauscher, H., Svendsen, C., Tsiliki, G., Zabeo, A., Hristozov, D., Stone, V., Wohlleben, W., 2021. How can we justify grouping of nanoforms for hazard assessment? Concepts and tools to quantify similarity. *NanoImpact* 100366.
- Jokar, M., Pedersen, G.A., Loeschner, K., 2017. Six open questions about the migration of engineered nano-objects from polymer-based food-contact materials: a review. *Food Additiv. Contamin. Part A* 34 (3), 434–450.
- Ministère de l'Environnement, D. L. É. E. D. L. M., 2015. *Éléments issus des déclarations des substances à l'état nanoparticulaire.* Exercice 2015.
- Nano-Enabled Packaging Market Share, Size, Trends, 2019. Industry analysis report by type (active, intelligent, others); By end-user (food and beverages, pharmaceutical, personal care, others); By regions: segment forecast, 2018–2026. *Pol. Mark. Res.*, PM1577
- Pantano, D., Neubauer, N., Navratilova, J., Scifo, L., Civardi, C., Stone, V., von der Kammer, F., Müller, P., Sobrido, M.S., Angeletti, B., Rose, J., Wohlleben, W., 2018. Transformations of Nanoenabled copper formulations govern release, antifungal effectiveness, and sustainability throughout the wood protection lifecycle. *Environ. Sci. Technol.* 52 (3), 1128–1138.
- Pillai, K.V., Gray, P.J., Tien, C.-C., Bleher, R., Sung, L.-P., Duncan, T.V., 2016. Environmental release of core–shell semiconductor nanocrystals from free-standing polymer nanocomposite films. *Environ. Sci. Nano* 3, 657–669.
- Platten, W.E., Sylvest, N., Warren, C., Arambewela, M., Harmon, S., Bradham, K., Rogers, K., Thomas, T., Luxton, T.P., 2016. Estimating dermal transfer of copper particles from the surfaces of pressure-treated lumber and implications for exposure. *Sci. Total Environ.* 548–549, 441–449.
- Sanchez-Garcia, M.D., Gimenez, E., Lagaron, J.M., 2008. Morphology and barrier properties of nanobiocomposites of poly(3-hydroxybutyrate) and layered silicates. *J. Appl. Polym. Sci.* 108 (5), 2787–2801.
- Schmidt, B., Katiyar, V., Plackett, D., Larsen, E.H., Gerds, N., Koch, C.B., Petersen, J.H., 2011. Migration of nanosized layered double hydroxide platelets from polylactide nanocomposite films. *Food Additiv. Contamin. Part A* 28 (7), 956–966.
- Shi, X., Gan, Z., 2007. Preparation and characterization of poly(propylene carbonate)/montmorillonite nanocomposites by solution intercalation. *Eur. Polym. J.* 43 (12), 4852–4858.
- Stark, W., Stoessel, P., Wohlleben, W., Hafner, A., 2015. Industrial applications of nanoparticles. *Chem. Soc. Rev.* 44 (16), 5793–5805.
- Störmer, A., Bott, J., Kemmer, D., Franz, R., 2017. Critical review of the migration potential of nanoparticles in food contact plastics. *Trends Food Sci. Technol.* 63, 39–50.
- Stratmann, H., Hellmund, M., Veith, U., End, N., Teubner, W., 2020. Indicators for lack of systemic availability of organic pigments. *Regul. Toxicol. Pharmacol.* 104719.
- Stratmann, H., Wohlleben, W., Wiemann, M., Vennemann, A., End, N., Veith, U., Ma-Hock, L., Landsiedel, R., 2021. Classes of organic pigments meet tentative PSLT criteria and lack toxicity in short-term inhalation studies. *Regul. Toxicol. Pharmacol.* 104988.
- Traas, L., Vanhauten, R., 2021. GRACIOUS Framework Blueprint, 1.0.
- Weiner, R.G., Sharma, A., Xu, H., Gray, P.J., Duncan, T.V., 2018. Assessment of mass transfer from poly(ethylene) nanocomposites containing Noble-metal nanoparticles: A systematic study of embedded particle stability. *ACS Appl. Nano Mat.* 1 (9), 5188–5196.
- Wigger, H., Wohlleben, W., Nowack, B., 2018. Redefining environmental nanomaterial flows: consequences of the regulatory nanomaterial definition on the results of environmental exposure models. *Environ. Sci. Nano* 5 (6), 1372–1385.
- Wohlleben, W., Punckt, C., Aghassi-Hagmann, J., Siebers, F., Menzel, F., Esken, D., Drexel, C.P., Zoz, H., Benz, H.U., Weier, A., 2017. Nanoenabled Products: Categories, Manufacture, and Applications. *Metrology and Standardization of Nanotechnology: Protocols and Industrial Innovations*, pp. 409–464.
- Zhang, Z., Kappenstein, O., Ebner, I., Ruggiero, E., Müller, P., Luch, A., Wohlleben, W., Haase, A., 2020. Investigating ion-release from nanocomposites in food simulant solutions: case studies contrasting kaolin, CaCO₃ and cu-phthalocyanine. *Food Packag. Shelf Life* 26, 100560.